

DOI: 10.1070/QEL16035

Fibre laser with a subterahertz repetition rate of ultrashort pulses in the telecom range

A.V. Andrianov, V.M. Mylnikov, M.Yu. Koptev, S.V. Muravyev, A.V. Kim

Abstract. **We have investigated a new fibre laser configuration for the generation of ultrashort pulses at a repetition rate far exceeding the fundamental cavity frequency. The laser configuration includes a nonlinear amplifying mirror as an artificial saturable absorber for mode locking and a spectral comb filter for pulse separation stabilisation. Generation of trains and sequences of ultrashort pulses at a repetition rate tunable in the range 8–200 GHz has been demonstrated experimentally. The pulses generated by the laser have been shown to retain an ordered, equidistant structure on a nanosecond timescale.**

Keywords: *fibre lasers, passive mode locking, ultrahigh repetition rate, telecom range.*

1. Introduction

The development of mode-locked lasers with a pulse repetition rate (PRR) exceeding 1 GHz and reaching subterahertz values has attracted a great deal of attention of researchers and potential users of such laser systems. This is primarily due to their possible applications in ultrahigh speed optical fibre telecommunication systems [1], frequency comb generation [2], materials processing [3] and terahertz radiation generation and detection [4]. In this respect, high-repetition-rate fibre lasers have considerable potential owing to their compact design, reliability and scalability to high average power, in combination with wide use of standard fibre-optic technologies and components in such lasers. Gaining insight into the physical mechanisms underlying the generation of high-repetition-rate ultrashort pulse (USP) trains is an important scientific issue. There is also considerable interest in the development of techniques for measuring parameters of such pulse trains.

To date, several approaches have been proposed for producing high-repetition-rate fibre lasers. One such approach relies on standard mechanisms of mode locking at the fundamental cavity round-trip frequency, with the cavity length made as short as possible. The limitation on the minimum fibre cavity length at which a gain coefficient sufficient for mode locking can be obtained makes it impossible to raise the PRR to above tens of gigahertz [5, 6].

Other approaches employ a rather long cavity, in which a train of closely spaced pulses is excited. Worthy of mention among them are methods based on mode locking at high fibre cavity harmonics [7, 8], the generation of trains of coupled dissipative solitons (soliton crystals) [9] and mode locking through dissipative four-wave mixing in the presence of a frequency comb filter [10, 11]. In addition, Yoshida et al. [12] and Dennis and Duling [13] proposed laser configurations that included a nonlinear amplifying loop mirror as an artificial saturable absorber and operated in the mode-locking regime with several pulses in the cavity. An increase in PRR was achieved by using an additional, short cavity [12] or an optical feedback loop, which ensured that part of the light reflected from the nonlinear mirror was returned to the main cavity with a time delay [13]. Mao et al. [14] have recently demonstrated a fibre laser mode-locked through nonlinear polarisation ellipse rotation, with an increase in repetition rate owing to the use of an intracavity Mach–Zehnder interferometer.

In this paper, we propose a new configuration of a fibre laser operating in the telecom range and capable of generating high-repetition-rate pulse trains. In this configuration, mode locking is achieved with a nonlinear amplifying loop mirror (NALM) having an inserted highly nonlinear fibre section, and the pulse spacing is stabilised by a frequency comb filter. This configuration has been prompted by the following considerations:

1. The nonlinear amplifying loop mirror as an artificial saturable absorber allows an all-fibre configuration to be created using standard telecommunications components and offers higher stability to external influences than does a saturable absorber based on nonlinear polarisation ellipse rotation [14]. Moreover, varying the coupling ratio of the fibre coupler and the fibre length, one can tune the nonlinear absorption of the loop mirror over a considerable range, which is difficult to achieve with the use of real saturable absorbers. It is worth noting that a nonlinear loop mirror can be made using polarisation-maintaining fibres, which allows one to develop a stable all-fibre high-repetition-rate USP source using standard telecommunications components.

2. Inserting a highly nonlinear fibre section ensures mode locking at very low pulse energies. This is particularly important for reaching high PRRs while maintaining the average power at a level acceptable for standard telecommunications components. Moreover, high nonlinearity allows the laser emission spectrum to be considerably extended.

3. The frequency comb filter is favourable for the generation of a set of equidistant modes, whose frequency spacing

A.V. Andrianov, M.Yu. Koptev, S.V. Muravyev, A.V. Kim Institute of Applied Physics, Russian Academy of Sciences, ul. Ul'yanova 46, 603950 Nizhnii Novgorod, Russia; e-mail: alex.v.andrianov@gmail.com;
V.M. Mylnikov Institute of Applied Physics, Russian Academy of Sciences, ul. Ul'yanova 46, 603950 Nizhnii Novgorod, Russia; Lobachevsky State University of Nizhnii Novgorod, prosp. Gagarina 23, 603950 Nizhnii Novgorod, Russia

Received 5 February 2016
Kvantovaya Elektronika **46** (4) 387–391 (2016)
Translated by O.M. Tsarev

determines the pulse separation T in a train: $T = 1/\Delta f$, where Δf is the mode frequency spacing. A Mach–Zehnder interferometer [14, 15], Fabry–Perot etalon [16], microcavities [17] and specially designed fibre Bragg gratings [18] can be used as filters.

In this report, we analyse two versions of the proposed configuration: with a Mach–Zehnder interferometer and with a low-finesse Fabry–Perot etalon as filters.

2. Configuration with a Fabry–Perot etalon

Figure 1 shows a detailed experimental laser configuration with a Fabry–Perot etalon. The gain medium used was a 1.5-m length of erbium-doped fibre pumped by a 550-mW single-mode laser diode at a wavelength of 975 nm through a wavelength division multiplexer (WDM). A 5-m-long section of a highly nonlinear fibre (nonlinearity coefficient $\gamma \sim 15$ W^{-1} km^{-1}) with low anomalous dispersion ($D = 2$ ps nm^{-1} $\times$ km^{-1}) was inserted into the nonlinear amplifying mirror. Fabry–Perot etalons of different thicknesses were placed in a gap in the fibre configuration. We used non-polarisation-maintaining fibres, so polarisation controllers were inserted into the nonlinear amplifying mirror and unidirectional propagation loop.

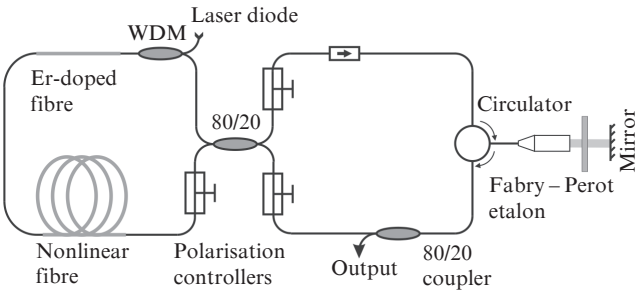

Figure 1. Schematic of the high-repetition-rate laser with a Fabry–Perot etalon.

With the controllers properly adjusted, we observed mode-locked laser operation with a large number of pulses circulating in the cavity. The average output power of the laser was about 4 mW. The minimum pulse energy for mode-locked laser operation was estimated at 1 pJ. Figure 2 shows the laser emission spectra obtained with Fabry–Perot etalons 1.8 mm (sapphire plate) and 0.5 mm (quartz glass plate) in thickness. It is seen that the spectra have the form of a set of narrow equidistant lines with a broad envelope, which corresponds to the spectrum of a solitary pulse. The spacing between the lines is determined by the thickness of the Fabry–Perot etalon and sets the pulse spacing corresponding to a frequency of 49 GHz (for the 1.8-mm-thick etalon, Fig. 2a) and 198 GHz (for the 0.5-mm-thick etalon, Fig. 2b). Note that the spectral modulation depth (on a logarithmic scale) and line shape vary little as the edges of the spectrum are approached, suggesting that the pulse train is coherent. The 3-dB bandwidth of the spectral envelope is about 15 nm and its 30-dB bandwidth is about 120 nm. The spectrum extends from 1460 to 1580 nm. These values exceed results reported for high-repetition-rate mode-locked lasers.

The photodiode we had was incapable of resolving individual pulses at such high repetition rates. The laser output

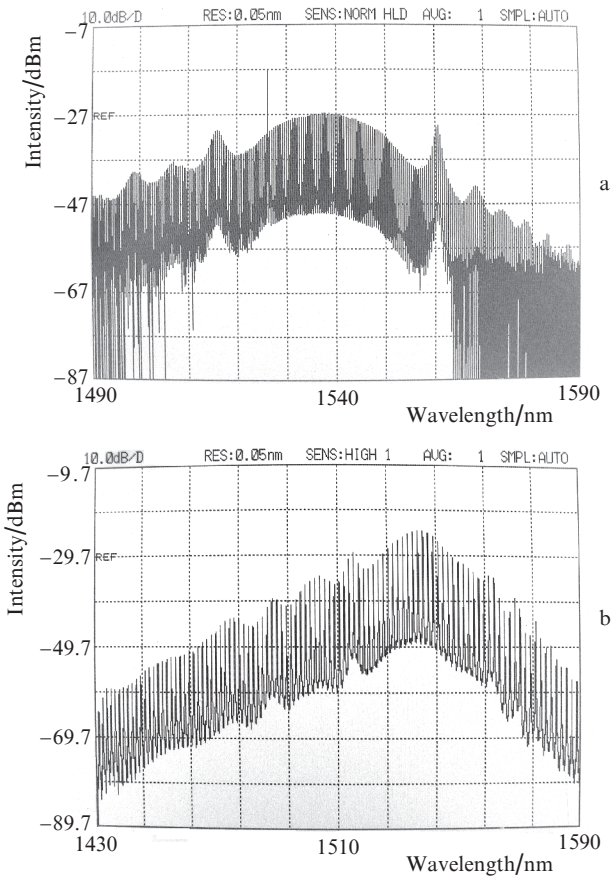

Figure 2. Laser emission spectra obtained with Fabry–Perot etalons (a) 1.8 and (b) 0.5 mm in thickness.

was measured using a photodiode with a pulse response time of about 250 ps and a 500-MHz oscilloscope (Tektronix TDS3052B, sampling rate of 5 GHz). Depending on the settings of the polarisation controllers, we observed oscilloscope traces in the form of both a train of 1- to 2-ns pulses (which corresponds to a high-repetition-rate sequence of bunches) and a constant signal, corresponding to a continuous sequence of high-frequency pulses (Fig. 3). It is of interest to note that the observed pulse train repetition time (about 3 ns) was substantially shorter than the cavity round-trip time (60 ns).

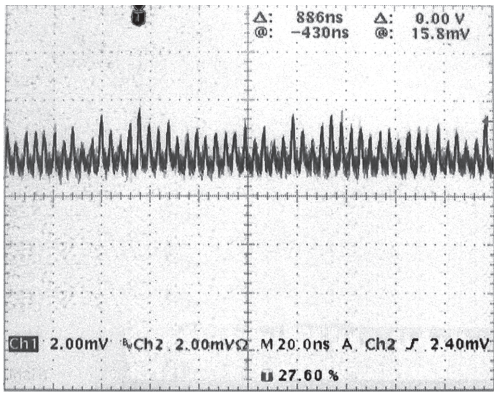

Figure 3. Oscilloscope trace of the photodiode signal in pulse train generation mode.

Thus, the pulse train repetition rate was also a harmonic of the fundamental cavity frequency.

3. Configuration with a Mach–Zehnder interferometer

Next, we analysed the laser configuration with a Mach–Zehnder interferometer used as a comb filter. The experimental laser configuration is shown in Fig. 4.

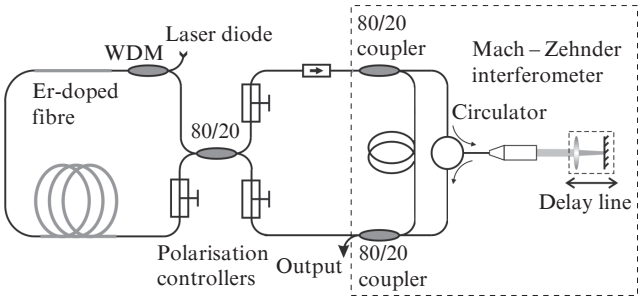

Figure 4. Schematic of the high-repetition-rate laser with a Mach–Zehnder interferometer.

The parameters of the active and passive fibres in this configuration were the same as in the laser with the Fabry–Perot etalons. One distinction was that a fibre Mach–Zehnder interferometer was used as a comb filter determining the pulse spacing. The interferometer included two fibre couplers: one of them split the light into two fibre channels, one of which had a variable length, and the other fibre coupler combined the signals from the channels. The fourth port of the latter coupler was used to outcouple part of the light from the cavity. To adjust the length of one of the interferometer arms, we developed a delay line that ensured a variable air gap in the fibre channel. The delay line comprised a fibre circulator, collimator and beam retroreflector mounted on a single-axis stage, which ensured translation along the beam. The beam retroreflector comprised a lens and a mirror placed at the lens focus, and formed a 1× telescope with image inversion. In contrast to a flat mirror, this configuration returned the collimated beam exactly at the angle of incidence (as measured from the incident beam direction), independent of slight tilts of the retroreflector system. This allowed us to reach high efficiency of beam recoupling back into the fibre even at large displacements by low-precision translation stages. With allowance for the losses in the circulator, collimator and uncoated lens, the transmission of the entire delay line exceeded 50% over the whole range of translation stage displacements (13 cm).

It is worth noting that the Mach–Zehnder interferometer (with a constant arm length difference) in this configuration can be made all-fibre, which will allow a high-repetition-rate all-fibre laser to be made using standard telecommunications components.

Figure 5 shows emission spectra of the laser in the mode-locking regime at different positions of the delay line and polarisation controllers. As in the case of the intracavity Fabry–Perot etalon, the spectra have the form of a set of narrow equidistant lines with a broad envelope. When the delay

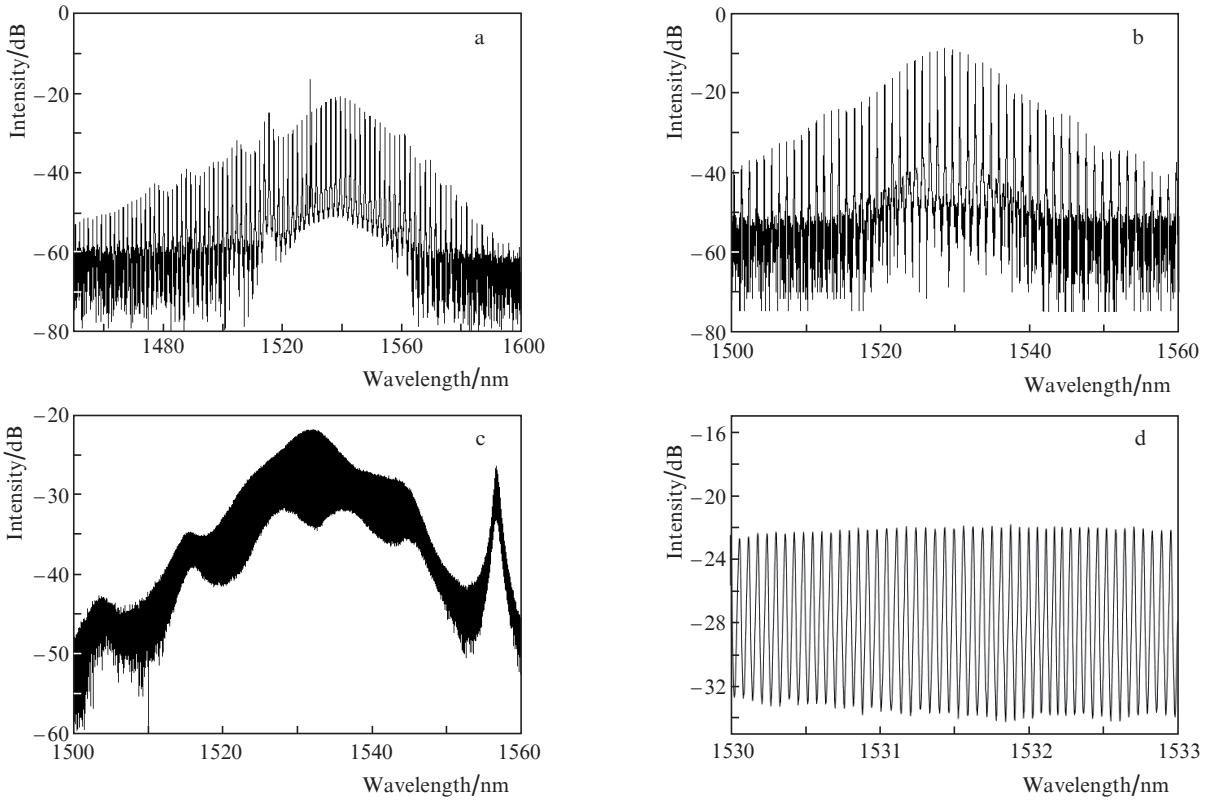

Figure 5. Laser emission spectra corresponding to PRRs of (a) 205, (b) 130 and (c) 7.8 GHz; (d) enlarged portion of the spectrum corresponding to a PRR of 7.8 GHz.

line was readjusted, the frequency spacing between the lines varied according to the formula $\Delta f = c/\Delta L$, where ΔL is the arm length difference of the Mach–Zehnder interferometer and c is the speed of light. The maximum PRR at which stable mode locking was observed in this configuration was 205 GHz.

Our experiments demonstrate that, to maintain the generation of a train of equidistant pulses, it is sufficient to ensure a small coupling ratio in the fibre couplers forming the Mach–Zehnder interferometer. The generation of pulse trains with a spacing determined by the arm length difference of the interferometer was observed at coupling ratios of 80/20 and 90/10 (the smaller part of the light was coupled into the delay line channel), so that after the channel combining the power of the additional pulse that passed through the delay line was 1%–3% of the main pulse power.

The temporal structure of the signal was studied using a photodiode with a pulse response time of about 100 ps and an Agilent Infinium 54854A oscilloscope (4-GHz bandwidth, 20-GHz sampling rate). Figure 6 shows oscilloscope traces of the photodiode signal under different laser operation conditions, corresponding to different PRRs. At mode spacings above 8 GHz, the signal was found to have the form of a sequence of pulse bunches propagating at the fundamental frequency. The cavity filling factor gradually increases with increasing length difference between the arms of the Mach– ehnder interferometer and, accordingly, with decreasing PRR. At PRRs under 8–20 GHz (depending on the settings of the polarisation controllers), there is no separation between pulse trains and a continuous sequence of bunches is generated.

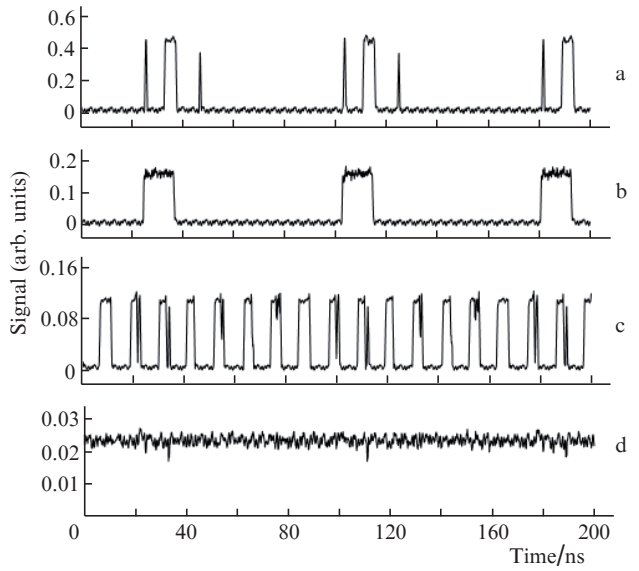

Figure 6. Oscilloscope traces of the photodiode signal under different laser operation conditions corresponding to PRRs of (a) 205, (b) 130, (c) 37 and (d) 7.8 GHz.

It is worth noting that mode locking was achieved not at any position of the delay line in the Mach–Zenhder interferometer, and moreover it was strongly influenced by the settings of the polarisation controllers. Nevertheless, after pulse train generation was achieved, smoothly varying the time delay led to a gradual, continuous variation in pulse spacing and the corresponding variation in pulse bunch duration.

To gain greater insight into the temporal structure of the pulse sequence, we performed autocorrelation measurements. To this end, we assembled an autocorrelator with a scan range of 100 ps. Before the autocorrelator input, the pulses were preamplified to an average power of about 400 mW. Note that, because of the long length of the active fibre in the amplifier, the pulse duration considerably increased due to dispersion-induced broadening.

Figure 7 shows autocorrelation traces recorded at different PRRs. In all cases, the autocorrelation function (ACF) has the form of a set of equidistant peaks, with a spacing determined by the inverse of the PRR. In addition, we recorded autocorrelation traces at PRRs of 37 and 20 GHz with one of the autocorrelator arms increased by 30 cm, which corresponded to a time delay of 1 ns (Figs 7b, 7c, dashed lines). It is seen that the autocorrelation trace recorded at the large arm length difference is similar in shape to that obtained at zero difference. This suggests that the pulses generated by the laser remain ordered and equidistant for at least 1 ns.

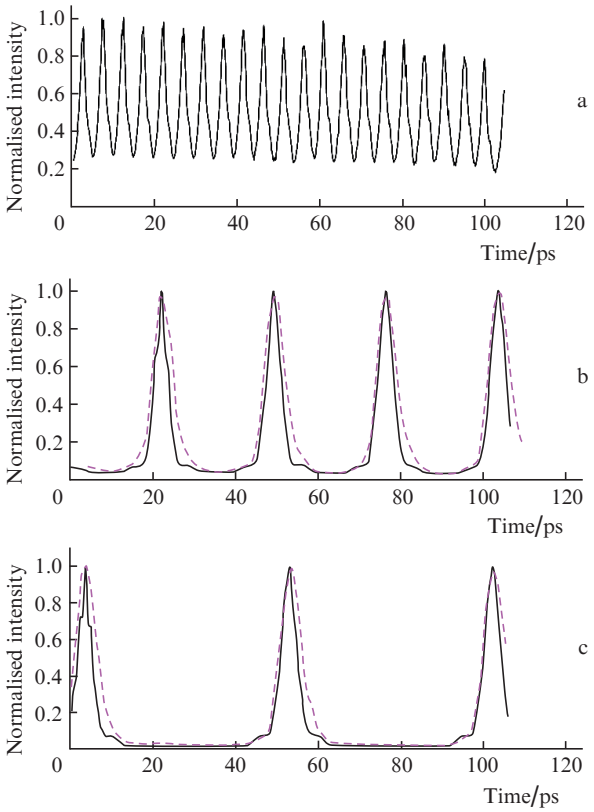

Figure 7. Autocorrelation traces of pulses at repetition rates of (a) 205, (b) 37 and (c) 20 GHz.

Thus, we have investigated a fibre laser for the generation of ultrashort pulses at a repetition rate many times higher than the fundamental cavity frequency. The laser configuration includes a nonlinear amplifying mirror as an artificial saturable absorber for mode locking and a spectral comb filter based on a Fabry–Perot etalon or Mach–Zenhder interferometer for pulse repetition time stabilisation. This configuration can be made all-fibre using standard telecommunications components and polarisation-maintaining fibres. A fibre laser has been demonstrated experimentally that generates bunches and sequences of ultrashort pulses at a repetition

rate tunable in the range 8–200 GHz. Autocorrelation measurements have shown that the pulses generated by the laser remain ordered and equidistant on a nanosecond timescale.

Acknowledgements. This work was supported by the Russian Foundation for Basic Research (Grant No. 14-29-08217 ofi_m).

References

1. Zhang Z.Y., Oehler A.E.H., Resan B., Kurmulis S., Zhou K.J., Wang Q., Mangold M., Suedmeyer T., Keller U., Weingarten K.J., Hogg R.A. *Sci. Rep*., **2**, 477 (2012).
2. Quinlan F., Ozharar S., Gee S., Delfyett P.J. *J. Opt. A: Pure Appl. Opt*., **11**, 103001 (2009).
3. Gattass R.R., Mazur E. *Nat. Photonics*, **2**, 219 (2008).
4. Chimot N., Mangeney J., Joulaud L., Crozat P., Bernas H., Blary K., Lampin J.F. *Appl. Phys. Lett*., **87**, 193510 (2005).
5. Martinez A., Yamashita S. *Opt. Express*, **19**, 6155 (2011).
6. Martinez A., Yamashita S. *Appl. Phys. Lett.*, **101**, 041118 (2012).
7. Grudinin A.B., Richardson D.J., Payne D.N. *Electron. Lett*., **29**, 1860 (1993).
8. Sobon G., Krzempek K., Kaczmarek P., Abramski K.M., Nikodem M. *Opt. Commun*., **284**, 4203 (2011).
9. Amrani F., Niang A., Salhi M., Komarov A., Leblond H., Sanchez F. *Opt. Lett.*, **36**, 4239 (2011).
10. Quiroga-Teixeiro M., Clausen C.B., Sorensen M.P., Christiansen P.L., Andrekson P.A. *J. Opt. Soc. Am. B*, **15**, 1315 (1998).
11. Sylvestre T., Coen S., Deparis O., Emplit P., Haelterman M. *Electron. Lett*., **37**, 881 (2001).
12. Yoshida E., Kimura Y., Nakazawa M. *Appl. Phys. Lett*., **60**, 932 (1992).
13. Dennis M.L., Duling I.N. *Electron. Lett*., **28**, 1894 (1992).
14. Mao D., Liu X., Sun Z., Lu H., Han D., Wang G., Wang F. *Sci. Rep*., **3**, 3223 (2013).
15. Lhermite J., Sabourdy D., Desfarges-Berthelemot A., Kermene V., Barthelemy A., Oudar J.L. *Opt. Lett*., **32**, 1734 (2007).
16. Yamashita S., Inoue Y., Hsu K., Kotake T., Yaguchi H., Tanaka D., Jablonski M., Set S.Y. *IEEE Photonics Technol. Lett*., **17**, 750 (2005).
17. Jyu S.S., Yang L.G., Wong C.Y., Yeh C.H., Chow C.W., Tsang H.K., Lai Y. *IEEE Photonics J*., **5**, 1502107 (2013).
18. Schröder J., Coen S., Vanholsbeeck F., Sylvestre T. *Opt. Lett*., **31**, 3489 (2006).